

NUMERICAL STUDY ON THE EFFECT OF A SUBMERGED BREAKWATER SEAWARD OF AN EXISTING BREAKWATER FOR CLIMATE CHANGE ADAPTATION

Athul Sasikumar¹ Arun Kamath² Onno Musch¹ Arne Erling Lothe¹ Hans Bihs²

¹Norconsult AS, Klæbuveien, Trondheim, Norway

² Department of Civil and Environmental Engineering, Norwegian University of Science and Technology (NTNU),
Trondheim, Norway

Email: athul.sasikumar@norconsult.com

ABSTRACT

In coastal areas, climate change is causing mean sea level rise and more frequent storm surge events. This means the breakwaters are expected to withstand the action of more severe incident waves and larger overtopping rates than they were designed for. Therefore, these impacts may have a negative effect on the functionality such as overtopping above the acceptable limits, in addition to stability of these structures. A breakwater which has been partly damaged by a storm stronger than the design storm has weak spots that can easily be damaged further. One way of protecting these breakwaters subjected to climate change is to build a submerged breakwater on the seaward side.

This study focuses on the use of numerical model for optimal dimension of a submerged breakwater to be used as a protective measure for an existing structure. Comparisons are made between transmission coefficient predicted in the numerical model and those calculated from different formulae in literature. The variation in transmission coefficient due to different relative submergence and relative width parameters for waves with different steepness is studied and curves showing the dependence of these parameters on wave transmission are made. These results are then used for a test case in Kiberg, Norway where a submerged breakwater is proposed in front of a existing damaged rubble mound breakwater. The optimal geometry generated on the basis of curves is then implemented in the local-scale finite element wave prediction model, CGWAVE.

INTRODUCTION

Submerged breakwaters have a great potential as a coastal protection structure as they can reduce the wave transmission with significant wave dissipation. These submerged breakwaters can enhance wave breaking, provide shoreline stability, reduce coastal erosion and preserve artificial nourishments implemented at the coast. These structures are most preferred where a moderate degree of energy transmission is acceptable. In some cases, where an existing emerged breakwater has been damaged due to a excessive loading, a submerged breakwater can be used in tandem to reduce the loads on the existing structure. A wave that becomes too steep when passing over the breakwater will break and some of the total energy will be dissipated. The area between the submerged breakwater and the main structure - the tranquillity zone - allows for energy dissipation. Thus, this tandem system results in waves with smaller heights reaching the main structure, which means that it may be designed with smaller armour units. This also means there is no need for further increase in the crest elevation of the existing breakwater which has been damaged, thereby maintaining the existing landscape and no additional visual intrusion. Another possible benefit is that this newly constructed porous breakwater can attract and preserve marine life around it.

One major challenge for these submerged structures are the tidal differences and storm surge events. These structures then become less effective due to a higher submergence on top of the structure. One way to tackle the higher transmission during storm surge is to have a wider breakwater crest. A wider

crest means a higher cost compared to narrow crested structures which limits their use in many situations.

The open source CFD model REEF3D is used in this study to simulate the wave transmission over a submerged breakwater. The breakwaters are modelled as porous structures and the flow inside the porous medium is solved using Volume averaged Reynolds-Averaged Navier–Stokes equations. This approach considers the porous medium as a continuous medium thereby eliminating the need for a detailed description of the complex geometry of the porous breakwaters. The numerical model uses a fifth-order WENO scheme for convection discretisation and a third order TVD Runge-Kutta scheme for time treatment of the RANS equations. Turbulence modelling is carried out using the two-equation $k-\omega$ model and the level set method is used to determine the free surface. A brief description about the equations and methods implemented in REEF3D is given in the following section. REEF3D has been successfully applied for a range of marine phenomena such as sediment transport [1], breaking wave forces [2], floating body dynamics [3] and sloshing [4]. The flow inside the porous medium is solved using Volume averaged Reynolds-Averaged Navier–Stokes equations (VRANS). VRANS equations consider the porous medium as a continuous medium and thereby eliminating the need for a detailed resolution of the individual rock components. The effects of turbulence within the porous medium are accounted for with the two equation $k-\omega$ turbulence model and the free surface is obtained using the level set method. The applied type of porosity model relies on empirical resistance coefficients which often need to be measured or calibrated. The numerical model REEF3D is validated for a 3D dam break case based on the experiments carried out by Lin (1999) [5].

Comparisons are made between transmission coefficient predicted in the numerical model and those calculated from different formulae in literature. The variation in transmission coefficient due to different relative submergence and relative width parameter for waves with different steepness is studied and curves showing the dependence of these parameters on wave transmission are made. The simulations in the numerical model are done using regular waves. The effect of slope and porosity of the submerged breakwater is not studied here since from literature those 2 parameters are found to have little influence on wave transmission [6] [7].

These results are then used for a test case in Kiberg, Norway where a submerged breakwater is proposed in front of a existing damaged rubble mound breakwater. The optimal geometry based on the curves generated is then implemented in the local-scale finite element wave prediction model, CGWAVE. It is a phase-resolving model based on mild slope equations (MSE) and uses a triangular finite-element formulation with grid sizes varying throughout the domain based on the local wavelength. The model allows one to specify the desired reflection properties along the coastline and other internal boundaries. The model

also uses a semi-circle as an open boundary to separate the model domain from the outer sea. Further details regarding the formulations and methods implemented in CGWAVE can be found in Panchang and Demirbilek (1998) [31]

NUMERICAL MODEL

Governing equations

In this study, the open source CFD model REEF3D is used to study the wave transmission over submerged breakwater. REEF3D uses the Reynolds-Averaged Navier-Stokes (RANS) equations along with the continuity equations to describe the fluid flow accurately.

$$\frac{\partial u_i}{\partial x_i} = 0 \quad (1)$$

$$\frac{\partial u_i}{\partial t} + u_j \frac{\partial u_i}{\partial x_j} = -\frac{1}{\rho} \frac{\partial p}{\partial x_i} + \frac{\partial}{\partial x_j} \left[(\nu + \nu_t) \left(\frac{\partial u_i}{\partial x_j} + \frac{\partial u_j}{\partial x_i} \right) \right] + g_i \quad (2)$$

In Eq. 1 and Eq. 2, u is the velocity averaged over time t , ρ is the fluid density, p is the pressure, ν is the kinematic viscosity, $\nu_t = k / \omega$ is the eddy viscosity, k is the turbulent kinetic energy, ω is the specific turbulent dissipation rate, t is time and g is the acceleration due to gravity. The projection method [8] is used for pressure treatment and the resulting Poisson pressure equation is solved using a preconditioned BiCGStab solver [9]. Turbulence is modelled using the two-equation $k-\omega$ model [10].

Additional limiters are included in the model to tackle the overproduction of turbulence at free surface [11] and eddy-viscosity [12] typical for oscillatory two-phase flow. The fifth-order Weighted Essentially Non-Oscillatory (WENO) scheme is employed to discretize the convection term of the RANS equations and the level-set equation, the turbulent kinetic energy and the specific turbulence dissipation rate [13].

The advancement in time is accomplished using a four-step scheme [14] with implicit treatment of convective and viscous terms. The Courant–Frederich–Lewy (CFL) condition for numerical stability is satisfied using a adaptive time stepping approach. The numerical model uses a uniform Cartesian grid for spatial discretization which simplifies the implementation of higher-order schemes. The staggered grid approach is used with pressure at the cell centers and velocities at the cell faces, providing a tight coupling between the pressure and the velocity. The code is fully parallelised using the MPI library and the numerical model can be executed on high performance computing systems with very good scaling.

Numerical Wave Tank

The numerical model REEF3D provides different methods for wave generation and absorption. One typical inlet boundaries for free surface flows are of Dirichlet type. This fixed value boundary condition is the simplest and the first to be implemented in most wave generating models, since theories give analytical expressions for free surface and the velocity distribution throughout the water column. To generate waves using this method, two variables for each time step are required. The first one is the free surface level at the generation boundary and the other one is velocity (horizontal and vertical components).

Relaxation methods can also be used for both wave generation and absorption. In this method, the analytical solution from wave theory is used to moderate the computationally generated waves in the wave tank. The computational value of velocity and free surface are taken from zero to the analytical values expected by wave theory in the wave generation zone. Similarly, at the numerical beach the computational value of velocity and free surface are brought to zero and all the energy is smoothly removed from the wave tank [15]. The values for velocity and free surface are moderated in the relaxation zones for wave generation and absorption using the following equation:

$$\begin{aligned} u_{relaxed} &= \Gamma(x)u_{analytical} + (1 - \Gamma(x))u_{computational} \\ \phi_{relaxed} &= \Gamma(x)\phi_{analytical} + (1 - \Gamma(x))\phi_{computational} \end{aligned} \quad (3)$$

In Eq. 3, $\Gamma(x)$ is the relaxation function and x is the coordinate along the x -axis scaled to the length of the relaxation zone. The relaxation function also absorbs reflections from the objects placed in the numerical wave tank, so that it does not affect wave generation and simulates a wave maker with active absorption. At the numerical beach, the computational values from the wave tank are reduced to zero so as to absorb the wave energy smoothly without spurious reflections from the beach. A no-slip boundary condition is applied on the bottom wall and on the surface of the objects in the tank and symmetry boundary conditions on the top of the numerical wave tank. The boundary conditions are enforced through the ghost cell immersed boundary method.

Level set method

The location of the free water surface is represented implicitly by the zero level set of the smooth signed distance function ϕ . This is modelled using the level set method given by Osher and Sethian(1988) [16]. The remaining domain, the level set function represents the closest distance of each point in the domain from the interface and the sign distinguishes the two fluids across the

interface. The level set function is defined as:

$$\phi(\vec{x}, t) \begin{cases} > 0 & \text{if } \vec{x} \text{ is in phase 1} \\ = 0 & \text{if } \vec{x} \text{ is at the interface} \\ < 0 & \text{if } \vec{x} \text{ is in phase 2} \end{cases} \quad (4)$$

The level set function is smooth across the interface and provides a sharp description of the free surface. The level set function is convected under the velocity field in the wave tank. The signed distance property of the function is lost by the motion of the free surface and it is restored by reinitializing the function after every iteration using the partial differential equations based on the procedure by Peng et al [17]. For the changes in interface (Γ) due to the changes in velocity field (\vec{u}) in the porous medium, a convection equation for the level set function is formulated in the VRANS framework as shown in Eq. 5.

$$\frac{\partial \phi}{\partial t} + \frac{u_j}{n} \frac{\partial \phi}{\partial x_j} = 0 \quad (5)$$

VRANS

REEF3D uses the Volume-averaged Reynolds-Averaged Navier-Stoke equations (VRANS) to solve the porous flow. It is important to accurately predict the porous flow in wave transmission over submerged breakwater especially when the crest level is close to the SWL. The averaging of RANS equations has been implemented based on the work done by Jensen et al. (2014) [18]. The incompressible RANS equations formulated with the continuity equation (Eq. 6) and momentum equation (Eq. 7) is averaged based on the volume averaging theorem [19].

$$\frac{\partial u_i}{\partial x_i} = 0 \quad (6)$$

$$\frac{\partial \rho u_i}{\partial t} + \frac{\partial \rho u_i u_j}{\partial x_j} = -\frac{\partial p}{\partial x_i} + g_j x_j \frac{\partial p}{\partial x_i} + \frac{\partial}{\partial x_i} \mu \left(\frac{\partial u_i}{\partial x_j} + \frac{\partial u_j}{\partial x_i} \right) \quad (7)$$

This continuity equation is averaged first with the assumption that the velocities on the solids are zero and resulting in Eq. 8. Here, $\langle \bar{u}_i \rangle$ is the velocity averaged over the volume and is called the filter velocity.

$$\frac{\partial \langle \bar{u}_i \rangle}{\partial x_i} = 0 \quad (8)$$

Next, each term in the momentum equation (Eq. 7) is volume averaged which results in Eq. 9 and Eq. 10.

$$(1 + C_m) \frac{\partial \rho \langle \bar{u}_i \rangle}{\partial t} + \frac{1}{n} \frac{\partial}{\partial x_j} \frac{\rho \bar{u}_i \bar{u}_j}{n} = \rightarrow -\frac{\partial \langle \bar{p} \rangle^f}{\partial x_j} + g_j x_j \frac{\partial \rho}{\partial x_i} + \frac{1}{n} \frac{\partial}{\partial x_j} \mu \left(\frac{\partial \bar{u}_i}{\partial x_j} + \frac{\partial \bar{u}_j}{\partial x_i} \right) + F_i \quad (9)$$

$$F_i = -a\rho \langle \bar{u}_i \rangle - b\rho \sqrt{\langle \bar{u}_j \rangle \langle \bar{u}_j \rangle \langle \bar{u}_i \rangle} \quad (10)$$

The term F_i on the right hand side of Eq. 9 represents the effect of turbulence in terms of additional resistance. This is modelled using the extended Darcy-Forcheimmer equation and is given by Eq. 10. Here a and b are the resistance coefficients and are defined by Eq. 11 and Eq. 12 [20]. In the relation for a and b , d_{50} is the grain diameter, n is the porosity and KC is the Keulegan-Carpenter number which represent the ratio between the turbulence and inertia effects. The coefficients α and β depends on the Reynolds number, shape of the stones, permeability and grade of porous material and have to be determined experimentally. The existing knowledge on the variation of resistance coefficients originates from theoretical considerations, physical experiments and numerical calibrations. The grain-fluid interaction is taken into account through the term C_m in Eq. 9. Here, C_m is the added mass coefficient which is described by the relation formulated (Eq. 13) by Van Gent (1992) [21].

$$a = \alpha \frac{(1-n)^2}{n^3} \frac{v}{\rho d_{50}^2} \quad (11)$$

$$b = \beta \left(1 + \frac{7.5}{KC} \right) \frac{(1-n)}{n^3} \frac{1}{d_{50}} \quad (12)$$

$$C_m = \gamma_p \frac{1-n}{n} \quad (13)$$

RESULTS

Validation of Numerical model - 3D Dam break

The VRANS equations used for solving the porous media flow need to be validated before any further study. A 3D dam break case is validated in REEF3D based on experiments conducted by Lin (1999) [5]. The resistance coefficients α and β need to be calibrated by completing a simulation matrix. The experiments were conducted inside a glass tank of 89.2 cm (l), 44 cm (w), 58

cm (h) and with a water depth of 25 cm (Fig. 1). The porous medium consisted of crushed rock with D_{n50} of 15.9 mm and porosity (n) of 0.49. Further details about the experiments can be found in Lin (1999) [5].

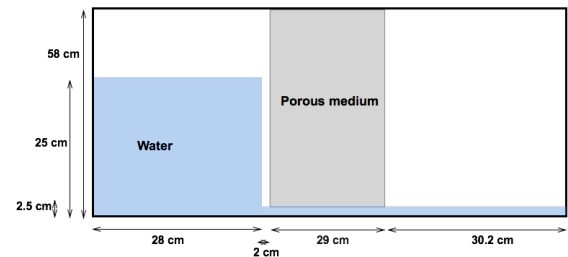


FIGURE 1. Setup for dam break

The experimental setup is replicated in the numerical wave tank by the same dimensions with a uniform grid size of $dx=0.5$ cm. The calibration of resistance coefficients is done by completing a simulation matrix, where the 2 coefficients are varied as $\alpha = [500, 650, 750, 1000, 2500]$ and $\beta = [1, 1.5, 2, 2.2, 3]$. The best match between experimental and numerical results was found for $\alpha=650$ and $\beta=2.2$ (Fig. 2). The agreement for this set of α and β coefficients is found to be very satisfactory. Small discrepancies are found for $t=0.4$ s and $t=0.6$ s which can be due to the difference of the initial flow conditions in the experiments and in the numerical model. In the experiments the water on the right side of the tank is blocked by a gate which is manually opened during the start of the experiments which results in water being rushed to the porous medium. In contrast, the gate is opened instantaneously in the numerical model. A very good agreement is found for $t>0.6$ s where the flow at the end which is also influenced by the reflected flow from the end of the tank. The interaction between the return flow and the porous medium is well represented in the model. The simulated case in the numerical model is shown in Fig. 3.

Submerged breakwaters - wave transmission formulae

There have been a number of laboratory experiments done to quantify the transmission coefficients (K_t) of submerged breakwaters. These formulae are derived from large data sets obtained from different laboratory experiments. These different design formulae indicates the importance of various variables in wave transmission. The physical variables that influence the transmission coefficient ($K_t=H_t/H_i$) are:

- d : submergence (water depth - crest height)
- b : crest width of breakwater
- h_c : crest height
- h : water depth in front of the structure
- m : front slope of the breakwater

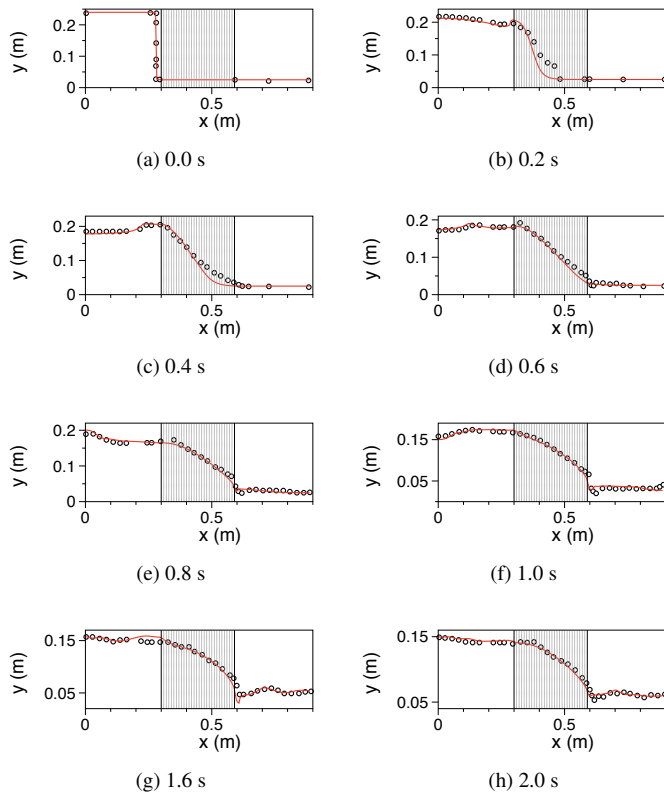


FIGURE 2. Comparison of free surface profiles for flow passing through porous medium - black dots indicate experimental results and red line indicate numerical results

- n : permeability
- D_{50} : nominal diameter of the outer layer
- H_i : incident wave height
- T : wave period
- L : wave length at local depth
- d/H_i : relative submergence
- b/L : relative width
- S_{op} : wave steepness

The wave transmission behind a submerged breakwater can be considered as a special case of low crested structure, with the crest level below the water level. Some of the semi-empirical expressions found in literature for the wave transmission over submerged breakwater are discussed here.

Arhens (1987) [22] investigated the wave transmission for low crested breakwaters at the US Army coastal engineering research centre. He proposed the following formulae (14) for low crested

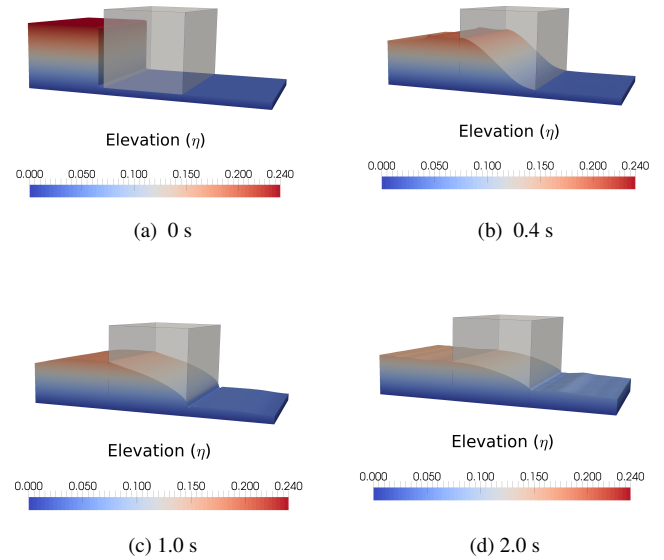


FIGURE 3. Free surface evolution for 3D Dam break

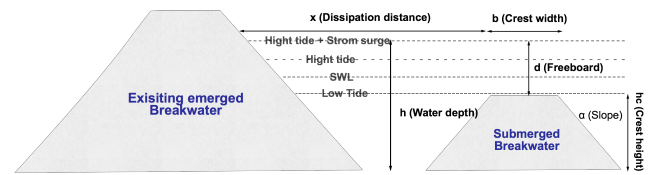


FIGURE 4. Definition sketch for breakwaters in tandem

breakwater, which is valid for a relative submergence, $d/H_i < 1$.

$$K_t = \frac{1}{\left\{ 1 + \left(1 - \frac{d}{h} \right)^{1.188} \left(\frac{F}{h \cdot L} \right)^{0.261} \cdot \exp \left[0.529 \left(-\frac{d}{H_i} \right) \right] \right\}} \cdot \frac{1}{0.00551 \left(\frac{F^{\frac{3}{2}}}{D_{50}^2 \cdot L} \right)} \quad (14)$$

Seabrook and Hall (1998) [6] performed 2-D and 3-D tests with irregular waves for various water depths, submergence, crest widths and incident wave conditions to study the transmission coefficient of submerged rubble mound breakwater. They identified that the important parameters influencing the transmission coefficient are the relative submergence (d/H_i) and crest width. Another important observations during their study is that the formulae proposed by Arhens (1987) [22] and van der Meer (1991) [23] is not suitable for calculating transmission coefficients for submerged breakwaters with wider crests. They proposed the following formulae (15) which includes a term for the

crest width.

$$K_t = 1 - \left[\exp\left(-0.65\frac{d}{H_i}\right) - 1.09\left(\frac{H_i}{b}\right) + 0.047\left(\frac{b.d}{L.D_{50}}\right) - 0.067\left(\frac{d.H_i}{b.D_{50}}\right) \right] \quad (15)$$

Eq. 15 is valid in the ranges of $0 \leq \frac{b.d}{L.D_{50}} \leq 7.08$ and $0 \leq \frac{d.H_i}{b.D_{50}} \leq 2.14$. Another semi-empirical relationship based on statistical analysis method was proposed by Siladharma and Hall (2003) [24] based on 3-D experimental study on wave transmission over submerged breakwaters.

$$K_t = -0.869 \exp\left(-\frac{d}{H_i}\right) + 1.049 \exp\left(-0.003\frac{b}{H_i}\right) - 0.026\frac{H_i}{b} \cdot \frac{d}{D_{50}} - 0.005\frac{b^2}{L.D_{50}} \quad (16)$$

The effect due to diffraction was removed from Eq. 16 in order to compare it with other formulae derived from 2-D studies. From Eq. 16, it can be seen that d/H_i is the governing parameter for wave transmission coefficient. Other parameters influencing the transmission coefficient are the relative crest width parameter (b/H_i), surface friction parameter (d/D_{50}) and an internal flow parameter ($b^2/L.D_{50}$).

Freibel and Harris (2003) developed a "best fit" empirical model from test data provided by Van der Meer (1998) [25], Daemen (1991) [26], Seelig (1980) [27], Daemrich and Kahle (1985) [28] and Seabrook (1997) [6]. This study also confirmed that the transmission coefficient is highly dependent on the relative submergence parameter (d/H_i).

$$K_t = -0.4969 \exp\left(\frac{d}{H_i}\right) - 0.0292\frac{b}{h} - 0.4257\left(1 - \frac{d}{h}\right) - 0.0696 \cdot \log\left(\frac{b}{L}\right) + 0.1359\left(\frac{d}{b}\right) + 1.0905 \quad (17)$$

Formulae vs. transmission coefficient (REEF3D)

The wave transmission over the submerged breakwater for a broad range of submergence is simulated in the numerical model and then compared with the K_t from empirical formulae mentioned in literature. The simulations in REEF3D are done for d/H_i ranging from 0 to 2.0, b/L of 0.1, 0.2 and for waves with a steepness (H_i/gT^2) of 0.006. The submerged breakwater is represented inside the 2D Numerical Wave Tank (NWT) of REEF3D. The 2D NWT is 40.0 m long and 1.0 m high with the breakwater centre being 17.0 m away from the wave generation. A uniform grid size of 1.0 cm is used in the entire domain which resulted in a total of 40000 cells. The type of waves generated here are the 5th-order Stokes waves with $H_i=0.2$ m, $T=1.8$ s, and the water

depth is set to be $d=0.5$ m.

In the numerical model, Dirichlet method is used for wave generation and for wave absorption at the other end of the NWT, active absorption methods based on shallow water theory is implemented. The active absorption at the end of the tank generates a wave opposite to the reflected one, effectively cancelling out the reflections. So this ensures the wave heights measured after the submerged breakwater are only the incoming transmitted wave height. The waves transmitted over the submerged breakwaters are highly irregular, so the transmitted wave height is defined as $H^{1/3}$ which is the average height of highest 1/3 of waves in the time series. The transmitted waves are measured at a distance of 2 times the water depth. The resistance coefficients are taken from existing literature [29].

- Armour stones: $D_{n50} = 0.0596$ m, $n = 0.5$, $\alpha = 1000$ and $\beta = 1.0$

Some formulae from the literature such as those formulated by Van der Meer (1991) [23], Daemen (1991) [26], d'Angremond (1996) [30] etc., have been excluded from this study due to their restricted case application and non-stability for broad crested and permanently submerged breakwaters. The different formulae in literature are results of laboratory experiments done with different conditions such as fully submerged or emerged structures, short or broad crested structure, breaking or non breaking waves etc. So it is important to check and restrict the application of these formulae based on the ranges suggested by the authors.

Fig. 5 illustrates the wave transmission computed in REEF3D compared to transmission coefficient computed using the empirical formulae. The numerically modelled wave transmission seem to fit best with Seabrook and Hall (1998) [6] and Siladharma and Hall (2003) [24]. The formulae of Seabrook and Hall (1998) [6] and Siladharma and Hall (2003) [24] involve the nominal diameter D_{50} of the armour layer of the breakwater, which includes the effect due to structural porosity. The formulae by Seabrook and Hall (1998) exclusively deals with submerged structures and is not applicable for emerged structures. The worst fit is found for comparison with Arhens, where transmission coefficient computed through Arhens equation seem to overpredict the transmitted wave height. This over-prediction of wave transmission has also been reported in literature by Seabrook and Hall (1998) [6]. Based on their extensive set of tests of wave transmission at submerged breakwaters, they claim that Arhens equations are not suitable to represent wave transmission for submerged structures especially where crest width are large. The formulae from Arhens (14) does not include the effect of crest width and thereby does not consider the changes in damping and shoaling caused by a larger width.

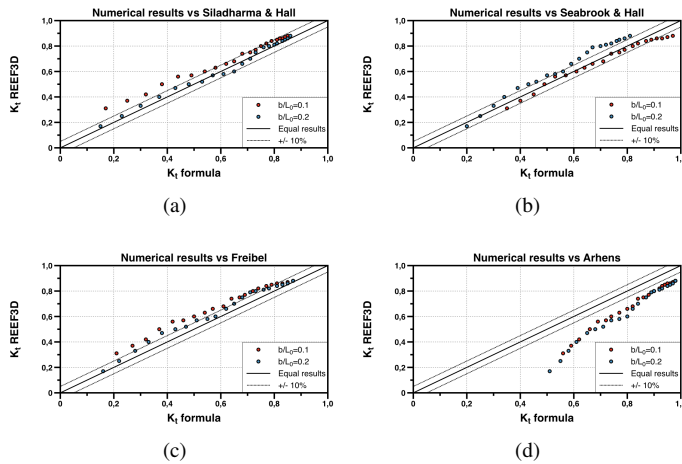


FIGURE 5. Comparison of transmission coefficients predicted by numerical model, $d/H_i = 0 - 2.0$, $b/L = 0.1-0.2$, $H_i/gT^2 = 0.006$

Relative submergence vs relative width

In order to study the influence of the relative submergence parameter and the relative width parameter, a wide range of crest heights and crest widths is tested in the numerical wave tank for waves with different steepness. An overview of the input parameters used in the study are shown in Table. 1

TABLE 1. Range of input parameters

Variable	Notation	Input
Incident wave height (m)	H_i	0.032 to 0.2
Wave period (s)	T	1.8
Water depth (m)	h	0.5
Nominal diameter (m)	D_{n50}	0.0596
Porosity	n	0.5
Slope	m	1:1.3
Crest height (m)	h_c	0.2 to 0.5
Crest width (m)	b	0.5 to 2.5
Submergence (m)	d	0.3 to 0
Relative submergence	d/H_i	0 to 1.6
Relative width	b/L	0.1 to 0.5
Steepness parameter	H_i/gT^2	0.001 to 0.01

Fig. 7 shows the trend of computed K_t for different steepness parameters (H_i/gT^2) ranging from 0.001 to 0.006. The most

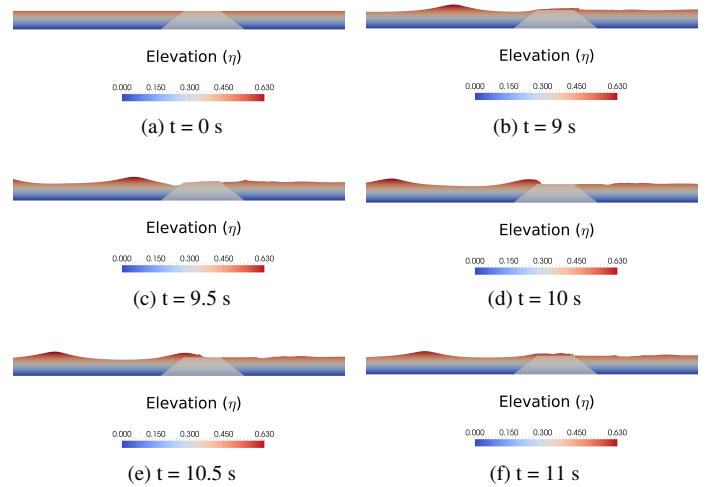


FIGURE 6. Wave transmission over submerged breakwater in REEF3D for different instance of time

dominant parameter determining the wave transmission is the relative submergence parameter (d/H_i). If this ratio is small, more damping of incoming waves is expected. An example simulation in REEF3D with a relative submergence parameter of zero is shown in Fig 6. The figure clearly shows the wave breaking process as the incoming wave approaches the submerged breakwater as most of the energy is damped out on top of the breakwater.

Another parameter of significant importance is the relative width parameter (b/L). A larger width means higher bottom friction as waves pass over the breakwater. Waves after breaking shoal more over the wider crest. For a given crest height and crest width, K_t decreases with increasing wave steepness. This is due to the fact the submerged breakwater breaks steeper waves than waves with a lower steepness coefficient, thereby increasing wave damping and wave height attenuation. This confirms the importance of crest width on the wave breaking and wave transmission. A large enough width is required for the submerged breakwater to efficiently break the waves and thereby reduce the transmitted wave height. A wider crest offers more frictional resistance to the waves at the bottom. In general, K_t decreases with an lower relative submergence and higher relative width parameter.

Test case: Submerged breakwater in Kiberg, Norway

A submerged breakwater has been proposed in front of existing rubble mound breakwater in Kiberg, Norway. The existing emerged breakwater has been damaged due to the focusing of waves towards the breakwater. So instead of repairing or raising the height of the damaged breakwaters, the possibility of using a submerged breakwater in front of the rubble mound breakwater

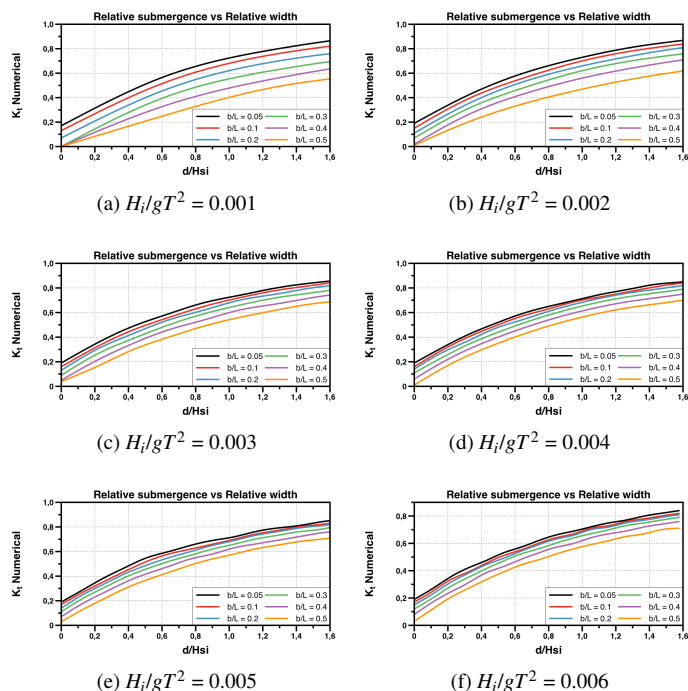


FIGURE 7. Effect of relative submergence (d/H_i and relative width (b/L) on transission coefficient (K_t), $d/H_i = 0 - 1.6$, $b/L = 0.1 - 0.5$; $H_i/gT^2 = 0.001 - 0.006$

is studied here. Fig. 8 shows the location of the test case in Norway where the red line shows the damaged section of existing breakwater and black line indicates the location of the proposed submerged breakwater. The design wave height and wave period have been chosen for a return period of 100 years and are derived from long term statistics from a nearby measuring station.

The submerged breakwater is proposed to stay submerged for the lowest water levels in order to avoid any kind of visual intrusions, in this case the LAT (Lowest Astronomical tide). This means that a higher submergence is expected at higher water levels (MSL or High water including storm surge). From the dependence curves made from numerical simulations, it is seen that the lowest transmission is seen for low relative submergence. So the crest height is set at 4 m (with reference to L.A.T), which means the $d/H_i = 0$ at LAT. For HAT (Highest Astronomical tide), a water level of 4 m above the submerged breakwater is expected which includes local storm surges as well. This is the most critical water level since higher transmissions are expected. The crest width is chosen to be 25 m, meaning a b/L of 0.1 for waves with a T_p of 15 s. A summary of design conditions for three different water levels is shown in Table. 2.

Since the highest transmission will be seen for the case with the highest submergence, the case with HAT will be considered here. For $H_i/gT^2 = 0.003$, $d/H_i = 0.6$ and $b/L = 0.1$ the transmission



FIGURE 8. Test case location: Kiberg, Norway.

TABLE 2. Design parameters for submerged breakwater in Kiberg

Variable	LAT	MSL	High water
Water depth, h	4.0 m	6.0 m	8.0 m
Wave height, H_i	3.0 m	5.0 m	6.5 m
Wave period, T_p	15 s	15 s	15 s
Crest height, h_c	4 m	4 m	4 m
Crest width, b	25 m	25 m	25 m
Submergence, d	0 m	2.0 m	4.0 m
Steepness parameter, H_i/gT^2	0.001	0.002	0.003
Relative submergence, d/H_i	0	0.4	0.6
Relative width, b/L	0.1	0.1	0.1

coefficient is found to be c.a. 0.55 (Fig. 7c). The selected breakwater geometry is implemented in the local-scale finite element wave prediction model, CGWAVE.

The submerged breakwater is modelled as a submerged bar in CGWAVE by making changes to the depth profile. An input wave height of 6.5 m and wave period of 15 s is used at the open boundary with a wave direction of 170° . There are some limitations when comparing the transmission coefficient obtained through REEF3D and CGWAVE. The submerged breakwater has a curved profile in CGWAVE, so the effective width felt by the waves will be different at different sections of breakwater. The effect of wave direction is not considered in REEF3D since the simulations were made in 2D. Similarly in REEF3D the effect

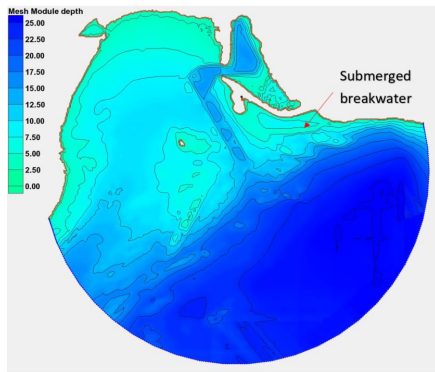


FIGURE 9. Depth profile for Kiberg, Norway.

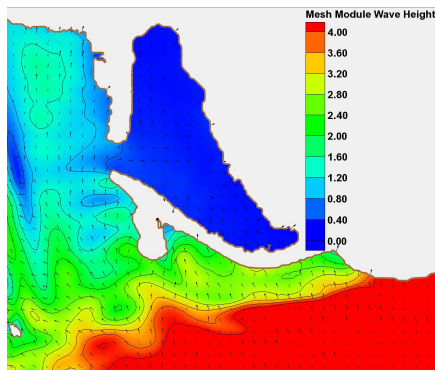


FIGURE 10. Wave height for situation with submerged breakwater Kiberg, Norway.

of damping due to porosity is included which is not included in CGWAVE. This will result in a somewhat higher wave transmission in the CGWAVE model. The transmission coefficient seen in CGWAVE will not have an effect due to diffraction since the submerged breakwater does not have open ends.

Fig. 9 shows the depth profile for the area of interest. The simulations are made using monochromatic waves in order to compare with transmission coefficients computed in REEF3D using regular waves. Fig. 10 show the wave condition near the existing emerged breakwater with a submerged breakwater in front. The effects of the submerged breakwater are clearly seen from Fig. 10 as a significant amount of energy is damped out and reflected back by the submerged breakwater. The input design wave height of 6.5 m is reduced to an average height of 4.5 m in front of the submerged breakwater due to changes in bathymetry. An average wave height of 2.8 m is found in the area between submerged and existing breakwater. This results in a K_t of 0.63 due to the submerged breakwater in CGWAVE which gives a satisfactory match with the K_t value obtained from REEF3D. The transmission coefficient is indeed a bit higher than REEF3D results mainly due to the fact that the porosity damping is not in-

cluded. For other water levels the transmission coefficient is expected to decrease.

CONCLUSIONS

The submerged breakwater with a large crest width and lower submergence successfully breaks steeper waves and dissipates wave energy. The wave transmission can vary significantly depending of the structural geometry, tidal level or changes in wave climate. In many situations due to aesthetic reasons it is important to have the breakwater submerged at all water levels. The transmission coefficient at the highest water levels should be used for design purposes. The selection of crest width of the submerged breakwater should be made as a function of cost. But the use of submerged breakwaters does provide significant reduction of wave energy and can reduce the extreme wave events impacting on the existing structure.

Transmission coefficients based on several published formulae in literature were compared to the numerical model REEF3D and were found to perform well within their stated limits. The best fit were found with Seabrook and Hall (1998) and Siladharmha and Hall (2003) and the worst fit is found for comparison with Arhens. The CGWAVE model based on mild slope equations gives satisfactory agreement to the transmission coefficient in REEF3D. The breakwaters in tandem may not always provide the least cost alternative in many situations considering the sort of materials and water depths but should be investigated as an alternative.

The plots showing the influence of crest width and height can be consulted for the preliminary selection of breakwater crest height and crest width for the specific design wave conditions. These figures should be part of further research to understand the influence of breakwater slope, porosity, incident wave direction and other relevant parameters.

ACKNOWLEDGEMENTS

This research was supported by the Norwegian coastal administration (NCA - <http://www.kystverket.no/>) and also in part with computational resources at NTNU provided by The Norwegian Metacenter for Computational Sciences (NOTUR), <http://www.notur.no>.

REFERENCES

- [1] Afzal, M. A., Bihs, H., Kamath, A., and Arntsen, Ø. A., 2014. "Three dimensional numerical modelling of pier scour under current and waves using level set method". In Proc. 33rd International Conference on Ocean, Offshore and Arctic Engineering, Volume 2: CFD and VIV, San Francisco, USA.
- [2] Kamath, A., Chella, M. A., Bihs, H., and Øivind A. Arntsen, 2016. "Breaking wave interaction with a vertical cylinder

- and the effect of breaker location". *Ocean Engineering*, **128**, pp. 105–115.
- [3] Bihs, H., and Kamath, A., 2016. "A combined level set/ghost cell immersed boundary representation for floating body simulations". *International Journal for Numerical Methods in Fluids*, pp. n/a–n/a.
- [4] Grotle, E., Bihs, H., Pedersen, E., and Æsøy, V., 2016. "Cfd simulations of non-linear sloshing in a rotating rectangular tank using the level set method". *ASME. International Conference on Offshore Mechanics and Arctic Engineering*.
- [5] Liu, P., Lin, P., Chang, K., and Sakakiyama, T., 1999. "Numerical modeling of wave interaction with porous structures.". *J. Waterw. Port Coast. Ocean Eng.*, **125**, pp. 322–330.
- [6] Seabrook, S., and Hall, K., 1998. "Wave transmission at submerged rubble mound breakwaters". *Proceedings of 26th International Conference of Coastal Engineering, ASCE*.
- [7] Dattatri, J., Raman, H., and Shankar, N. J., 1979. "Performance characteristics of submerged breakwaters". *Coastal Engineering*.
- [8] Chorin, A., 1968. "Numerical solution of the Navier-Stokes equations". *Mathematics of Computation*, **22**, pp. 745–762.
- [9] Van der Vorst, H., 1992. "Bi-gstab: A fast and smoothly converging variant of bi-cg for the solution of nonsymmetric linear systems". *SIAM J. Sci. Stat. Comput.*, **13**, pp. 631–644.
- [10] Wilcox, D. C., 1994. *Turbulence modeling for CFD*. DCW Industries Inc., La Canada, California.
- [11] Naot, D., and Rodi, W., 1982. "Calculation of secondary currents in channel flow". *Journal of the Hydraulic Division, ASCE*, **108**(8), pp. 948–968.
- [12] Bradshaw, P., Ferriss, D. H., and Atwell, N. P., 1967. "Calculation of boundary layer development using the turbulent energy equation". *Journal of Fluid Mechanics*, **28**, pp. 593–616.
- [13] Jiang, G. S., and Shu, C. W., 1996. "Efficient implementation of weighted ENO schemes". *Journal of Computational Physics*, **126**, pp. 202–228.
- [14] Choi, H., and Moin, P., 1994. "Effects of the computational time step on numerical solutions of turbulent flow". *Journal of Computational Physics*, **113**, pp. 1–4.
- [15] Jacobsen, N. G., Fuhrman, D. R., and Fredsøe, J., 2011. "A wave generation toolbox for the open-source CFD library: OpenFOAM". *International Journal for Numerical Methods in Fluids*, **70**(9), pp. 1073–1088.
- [16] Osher, S., and Sethian, J. A., 1988. "Fronts propagating with curvature- dependent speed: algorithms based on Hamilton-Jacobi formulations". *Journal of Computational Physics*, **79**, pp. 12–49.
- [17] Peng, D., Merriman, B., Osher, S., Zhao, H., and Kang, M., 1999. "A PDE-based fast local level set method". *Journal of Computational Physics*, **155**, pp. 410–438.
- [18] Jensen, B., Jacobsen, N., and Christensen, E., 2014. "Investigations on the porous media equations and resistance coefficients for coastal structures.". *Coastal Engineering*, **84**, pp. 56–72.
- [19] Howes, F., and Whitaker, S., 1984. "The spatial averaging theorem revisited". *Chemical Engineering Science*, **40**, p. 1387–1392.
- [20] van Gent, M., 1992. "Stationary and oscillatory flow through coarse porous media.". *Communications on hydraulic and geotechnical engineering, Delft University of Technology, Delft (The Netherlands)*, **93-9**, pp. 42–46.
- [21] van Gent, M., 1992. "Formulae to describe porous flow.". *Communications on hydraulic and geotechnical engineering, Delft University of Technology, Delft (The Netherlands)*, **92-2**, pp. 42–46.
- [22] Ahrens, J. P., 1987. Characteristics of reef breakwaters. Tech. rep., Coastal Engineering Research Center.
- [23] Van der Meer, J., 1991. "Stability and transmission at low-crested structures". *Delft Hydraulics Publication, Delft University of Technology, Delft (The Netherlands)*.
- [24] Siladharma, I., and Hall, K., 2003. "Diffraction effect on wave transmission at submerged breakwaters.". *Technical Report, University of Technology, Bali*, pp. 1–12.
- [25] Van der Meer, J., 1998. "Rock slopes and gravel beaches under wave attack". *Doctoral thesis, Delft University of Technology, Delft (The Netherlands)*.
- [26] Daemen, I., 1991. "Wave transmission at low-crested structures". *M.Sc. Thesis Delft, University of Technology, Delft Hydraulics(H462)*.
- [27] Seelig, W., 1980. "Estimation of wave transmission coefficients for overtopping of impermeable breakwaters". *CERC, Coastal Engineering Technical Aid*.
- [28] Daemrich, K., and Kahle, W., 1985. "Schutzwirkung von unterwasser wellenbrechern unter dem einfluss unregelmässiger seegangswellen". *Technical Report, Franzius-Institut für Wasserbau und Küsteningenieurwesen*, **116**(61).
- [29] Troch, P., 2000. "Experimentele studie en numerieke modellering van golfinteractie met stortsteengolfbrekers". *Ph.D. thesis. Faculty of Engineering and Architecture, Ghent University, Ghent (Belgium)*, **0**, pp. 131–160.
- [30] d'Angremond K, J., van der Meer, and de Jong, R., 1996. "Wave transmission at low-crested structures". *Proc. 25th Int. Conf. on Coastal Engineering, ASCE*, pp. 3305–3318.
- [31] Demirbilek, Z., and Panchang, V., 1998. "Cgwave: A coastal surface water wave model of the mild slope equation". *U.S. Army Corps of Engineers*.